# STAR TRACKER OPERATION IN A HIGH DENSITY PROTON FIELD

Kenneth J. Miklus, Frank Kissh, and David J.Flynn
Hughes Danbury Optical Systems, Inc.



## ABSTRACT

Algorithms that reject transient signals due to proton effects on charge coupled device (CCD) sensors have been implemented in the HDOS ASTRA-1 Star Trackers to be flown on the TOPEX mission scheduled for launch in July 1992. A unique technique for simulating a proton-rich environment to test trackers is described, as well as the test results obtained.

Solar flares or an orbit that passes through the South Atlantic Anomaly can subject the vehicle to very high proton flux levels. There are three ways in which spurious proton generated signals can impact tracker performance: the many false signals can prevent or extend the time to acquire a star; a proton-generated signal can compromise the accuracy of the star's reported magnitude and position; and the tracked star can be lost, requiring reacquisition. Tests simulating a proton-rich environment were performed on two ASTRA-1 Star Trackers utilizing these new algorithms. There were no false acquisitions, no lost stars, and a significant reduction in reported position errors due to these improvements.

## STAR TRACKER OPERATION IN A HIGH DENSITY PROTON FIELD

Star sensors have been utilized in high-accuracy attitude determination systems since the early 1960's, providing precise measurement of the position and magnitude of stars in the sensor's field of view (FOV). As applications continue to demand higher performance, the effects of a natural or enhanced radiation environment need to be accommodated by the star sensor's design. HDOS recently delivered two star trackers for the TOPEX/Poseidon mission which is scheduled for launch in July 1992. These enhanced trackers contain an efficient mix of hardware and firmware that permits effective acquisition and tracking throughout their orbit, which includes extensive exposure to the transient rich environment of the South Atlantic Anomaly. This paper discusses the algorithms employed, the environment simulated, and the results of the tests performed, demonstrating successful operation in a proton-rich environment.

## BACKGROUND

State-of-the-art star sensors (see Figure 1) have recently benefited from two major technological developments, the CCD detector and the microprocessor. The heart of the current HDOS ASTRA star sensors is the RCA 504 CCD, a 256 × 403 pixel array which operates in the frame transfer mode. The thinned, backside illuminated device provides high quantum efficiency in the visible range. A thermoelectric cooler is used in the ASTRA-1 sensors to provide low noise operation in harsh environments. Fitted with a wide FOV (7×9 degree) color corrected lens, the ASTRA star sensors can provide position accuracy to 10 arc-seconds or better, and sensitivity down to a visual magnitude of 6. The HDOS ASTRA star sensors also utilize a versatile 16-bit microprocessor. Acquisition and tracking, centroid determination and correction, debris and transient event discrimination, and self-test functions are performed autonomously by the microprocessor. This design provides a flexible interface and reduces the computation burden on the host computer.

Star sensors utilizing mosaic CCD arrays can be separated into two classes: star trackers and star mappers. Star trackers have two distinct functional modes: acquisition and track. During acquisition, the sensor field of view is searched for valid targets. High-pass spatial filtering and pixel amplitude thresholding are often used to limit the amount of data saved each frame. Data from multiple frames can be used during acquisition to discriminate valid stars from debris and transient events. Once a star has been acquired, the sensor enters the track mode. During the track mode, data from previous frames is used to estimate the current position of

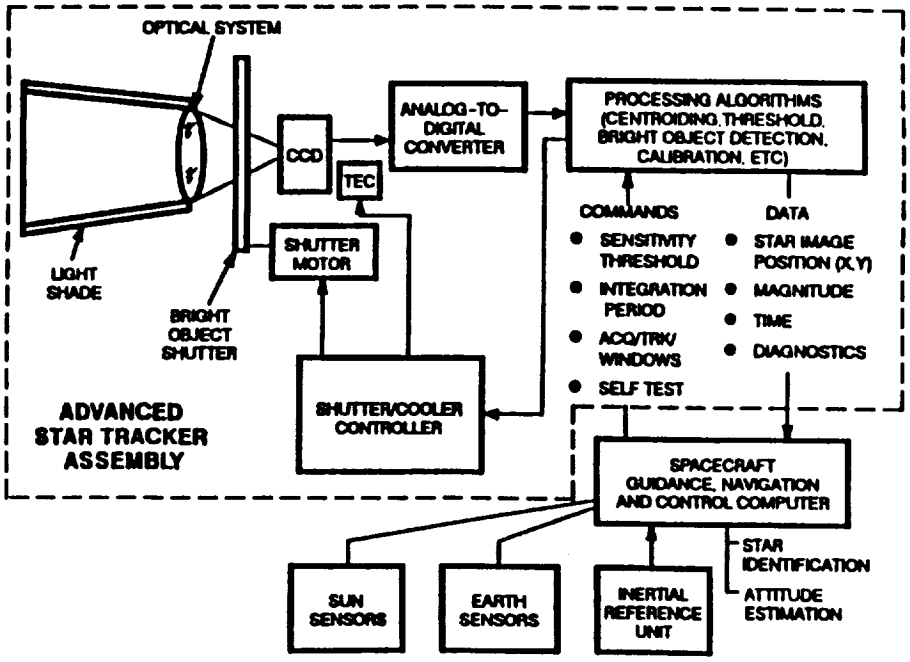


**Figure 1. Functional Diagram of the Advanced Star Tracker (ASTRA).**

the star. A reduced field surrounding the star is then read, processed, and the magnitude and position of the star are output to the host. The HDOS ASTRA-1 built for the TOPEX/Poseidon mission is an example of a star tracker. The ASTRA Star Tracker currently being built for Space Station Freedom will operate as four virtual star trackers allowing simultaneous acquisition and tracking of up to four stars.

Star mappers acquire stars throughout the total sensor field of view and report their magnitude and position each frame. High pass filtering and pixel amplitude thresholding are used to limit the amount of data that must be processed each frame. Normally, information is not saved from frame to frame. The HDOS ASTRA-2 built for the JH/APL START experiment[1] is an example of a star mapper. It outputs the position and magnitude of up to five stars at a 10 Hz update rate.

Trackers have a number of functional advantages over star mappers when operating in a transient event-rich environment. Once a star tracker has acquired a star, only a small fixed number of pixels must be read, stored, and processed each frame. A star mapper must process the entire CCD array each frame and the number of transient events will impact the amount of data that must be processed. By using data from multiple frames, star trackers can discriminate between stars (with predictable magnitudes and positions) and transient events during acquisition. Using magnitude and position data from previous frames during track mode also allows a star tracker to determine if a transient event has corrupted the reported magnitude and position data. Star mappers do not store information from previous frames and cannot discriminate between transient events and valid targets; this task must be performed by the host. Star mappers can also report a different set of stars each frame which requires identification of stars each frame. In a star tracker system, once a valid star has been identified, there is no need for the host to re-identify a star so long as it remains in track.

## THE ENVIRONMENT

For a star sensor to operate in a natural or enhanced radiation environment, the effects of radiation damage and radiation induced noise events on the CCD must be addressed. Space radiation that will interact with the CCD can be divided into two major groups, trapped particles and solar protons.[2,3] Trapped particles are protons and electrons trapped in the magnetic fields surrounding the earth. The energy and fluence profiles will

vary with the altitude and inclination of the orbit. In low earth orbits, anomalies at the poles and off the coast of Brazil (the South Atlantic Anomaly) can result in high fluxes of energetic protons. Solar protons are emitted during solar flares which occur randomly. Intense solar flares occur about every 11 years. At high altitudes, i.e. geostationary orbit, solar protons can dominate, with fluxes sometimes orders of magnitude greater than the trapped particle radiation. HDOS has developed the capability to evaluate the radiation environment in space and its impact on sensor systems for given orbits. These models are based on the RADBELT AP-8, AE-8 radiation environment data supplied by NASA-GSFC.

The effects of radiation damage in CCDs have been the focus of much recent work.[4] HDOS has developed the tools required to model the end-of-life performance of CCD detectors, and has also performed experiments to measure these effects on irradiated devices. The primary concern of this paper is the effect of transient noise events that occur when high energy particles impact the CCD. Charged particles interact directly with the CCD pixels, causing a random series of ionization events. These events can be localized to within a few pixels or can result in streaks, depending on the angle of incidence of the particle, the geometry of the device, and the energy of the particle.[5,6] A large number of events in the sensor field of view can interfere with the operation of the sensor. If the system must operate in a high density proton environment, a method to reduce the impact of these events on the sensor operation is required. The most obvious solution is to increase the shielding around the CCD to reduce the number of events. However, this will increase system size and weight. A more elegant solution is to apply real-time processing to reject these transient events.

Transient events can degrade a star tracker's performance in a number of ways. During acquisition, transient events can be acquired falsely or can impede acquisition of a valid target. During track, transient events can corrupt position and magnitude data or can result in the sensor dropping a valid star track. For the TOPEX mission, Fairchild Space Co.[7] determined that the star tracker must operate with up to 150 transient events in the sensor FOV per frame, 100 milliseconds. All of these events were assumed to be indistinguishable from real stars to the CCD. Since these transient events were independent of one another their position and magnitude were random and uniformly distributed over the CCD array.

The system had to meet the following requirements:

- Acquire and track stars with up to 150 transient events per frame
- Acquire and track stars moving up to 0.3 degree/second
- Probability of acquiring a valid star within 22 seconds is 95%
- Alert host if data has been corrupted
- Maintain track of valid stars during proton event disturbances.

## ALGORITHM IMPLEMENTATION

Any solution is dependent on determining what information is available to discriminate between transient events and valid stars. Star image size is a function of the point spread of the optics and the motion and jitter of the spacecraft. Therefore, bounds can be placed on the size of valid targets and single pixel upsets and events that result in long streaks can be rejected. Proton events only last for one frame. Since they are independent of one another, the position and magnitudes of the proton events randomly change from frame to frame. Positions of the star images on the array are determined by the dynamics of the spacecraft and therefore change systematically from frame to frame. By applying spatial and magnitude filtering, we can reject transient events. The probability of transient events passing this filter will be a function of the number of transient events per frame and the size of the discrimination windows. The line-of-sight (LOS) motion requirement (up to 0.3 degree/second) thus determines the minimum spatial window to be used. The size of the magnitude window is determined by the tracker's predicted error in determining star magnitude. Once a star is acquired, magnitude can be checked to determine if a transient event is contiguous with the star image, causing an error in the centroid of the image and in its reported magnitude.

Our selected approach was to limit the data processing load during each tracker frame when in the acquisition mode to be consistent with existing hardware capabilities. The tracker FOV was divided into 19 acquisition bands (19 pixel rows by 403 pixel columns). The bands were stacked in the row direction with a small overlap and the search for a star confined to one band at a time. If the acquisition sequence fails to find a star in the current band, the tracker sequences to the next band and searches for a valid star. This sequence continues until the tracker acquires a star in one of the bands and transitions to track mode. If the entire FOV is searched unsuccessfully, the sequence is repeated.

The acquisition sequence consists of two acquisition states (A1 and A2) and five validation states (H1 through H5). Each state takes one tracker frame to implement.

The acquisition sequence searches an acquisition band to determine if any group of pixels with signal exceeding a threshold exists that could quality as a star. If no such group exists the tracker transfers to the next acquisition band and the sequence is repeated. If candidate stars are found in the A1 state, the tracker enters the A2 state. If any of the candidate stars identified in A1 is also found in A2, the tracker goes into the validation phase of the acquisition sequence. During validation states, the tracker continues to evaluate the candidate star's characteristics for temporal and spatial consistency. Upon transition to the track state, sufficient history has been established so that it is highly probable that the group represents a valid star and is not caused by transient events. If the star is not confirmed in any of the validation states the tracker increments to the next acquisition band and the acquisition sequence is continued.

Upon transition to track, a small track window is defined which is centered about the last validated star position. The window position is updated each frame to track the updated star position. The window is made small enough to limit the data processing load and exclude the majority of transient proton signals; but it is large enough to account for vehicle LOS rates.

The track window is scanned in a raster fashion each frame, and the magnitude and position characteristics of the candidate star are evaluated. If the star is evaluated as a "valid" star, the centroid data and star magnitude data are sent to the host and a bit is set in the data word that indicates the data is valid. If no valid star is found in the track window after multiple attempts to recover from proton hits, the star is considered lost and the tracker reverts to the acquisition mode.

## TEST METHOD

The CCD's inability to distinquish between proton or photon generated-signals was utilized to test the tracker with the proton flux improvements. A Scene Simulator (SS) concept was implemented. Scenes consisting of point sources of light were generated on a computer monitor. The point sources were collimated and then imaged by the tracker on its CCD detector. The signals generated in this fashion at the CCD could be considered as having been generated by either protons or stars. This technique achieved complete control of the interactions between a simulated star and simulated proton events.

The SS equipment shown in Figure 2 consisted of a VGA monochrome monitor and a personal computer (PC) with a 386 processor running at 25 MHz. The monitor was positioned at the focal plane of an achromatic collimating lens with a focal length (FL) of 1185 mm. The scene was generated by commanding 150 monitor pixels on, to serve as "proton" sources, and one pixel to serve as a "star". The intensity of each monitor pixel was controlled by the SS software. The collimated light from each monitor pixel was imaged by the tracker optics on its CCD detector. The tracker optics had an FL of 41 mm which imaged the monitor pixels at the CCD detector, resulting in a demagnification factor of 29. All images at the tracker, simulated protons as well as simulated stars, were equivalent in size to predictions for a valid star in orbit, i.e. between two and 25 CCD pixels. The angular FOV that the monitor accommodated exceeded the 9×7 degree FOV of the tracker.

To ensure a worst-case test scenario, all proton events were sized (in pixels) within the range considered by the tracker to be acceptable stars. Figure 3 (frames 299 and 300) shows the excellent image size achieved with the Scene Simulator.

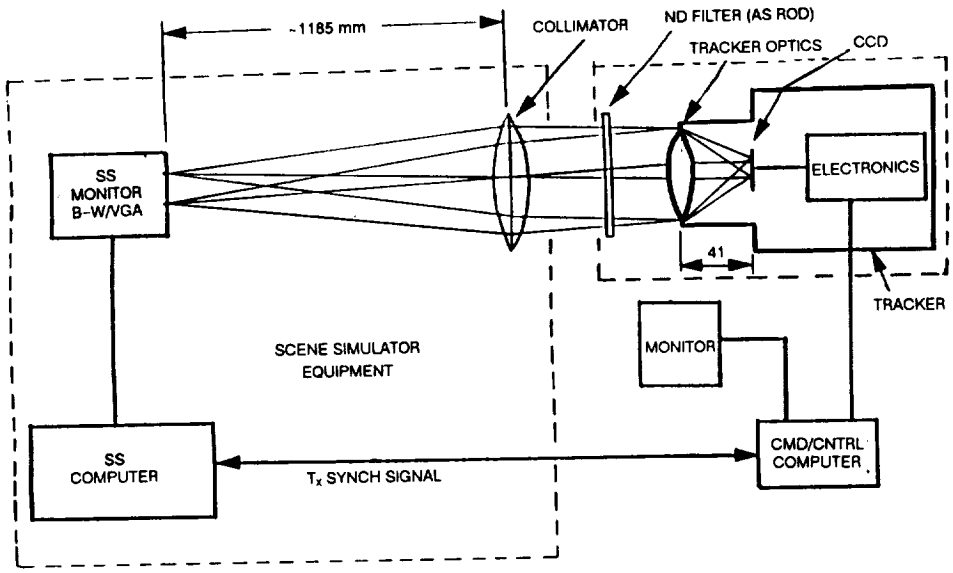


**Figure 2. Configuration for Simulation of Stars and Proton Events in a Laboratory Environment.**

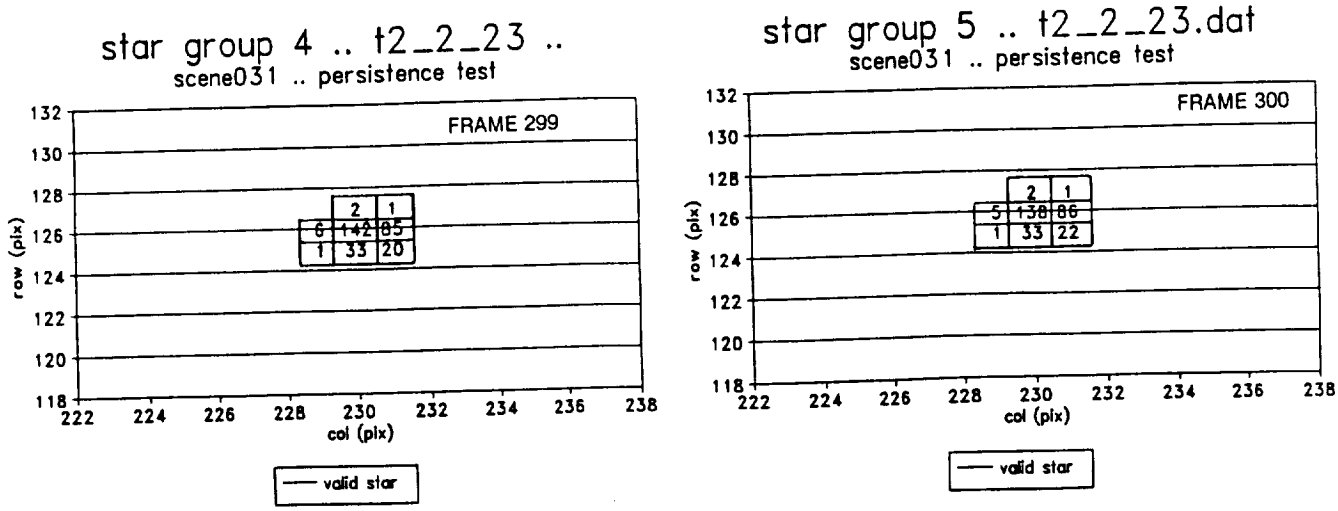


**Figure 3. Excellent Image Properties Were Achieved with the Scene Simulator (Mi~3.7).**

To limit simulated proton signals to one tracker frame, the generated scene display was synchronized with the 10 Hz frame rate of the tracker. This synchronization was mandatory because a star will be imaged at a spatially consistent location during successive tracker frames, whereas a proton signal will be transitory both spatially and temporally.

## TESTS RESULTS

The tests described were designed to verify three basic aspects of the tracker software performance in a proton-rich field, specifically:

- A star being tracked will not be lost as a result of the proton events
- Acquisition of a valid star will occur within 22 seconds of the start of the search and star position
- Magnitude data corrupted by proton events will be identified for the host.

The scene simulator technique was especially useful since the intensities and positions of the simulated protons could be varied by the software to have any desired relationship to the simulated star. In all, 14 unique scenarios were used to test the response of the tracker to various combinations of "proton" influences on tracker performance. Generally the scenes simulated conditions of near or direct proton hits on the star position. In addition a "no stars" scene was used to verify that the tracker software was not fooled by the "proton" signals and did not erroneously report star acquisitions. Both moving and stationary stars were simulated.

Each test scene scenario always consisted of 150 simulated protons and one simulated star. The simulated proton positions were generated in a random fashion in the tracker's FOV. Consistent with Fairchild's radiation analysis/specifications, 35 of the simulated proton signals were at an equivalent star Instrument Magnitude (Mi) of 3.2; 115 ranged between the equivalent Mi of 3.7 and 5. The simulated star was set at Mi = 3.7. Generally the "star" in the scenes was not subjected to random "proton" influences. Each scene was carefully designed to introduce specific and periodic occurrences of "proton/star" interactions so that tracker software processes could be evaluated. Completely random occurrences of "proton/star" interactions were used to gather statistical information regarding frequency of "star" disturbances, to ensure that the three primary performance requirements were met and that interacting events did not cause unanticipated results.

The results of a test designed to demonstrate ASTRA's capability to reject "protons" during the star acquisition sequence are shown in Figure 4. The particular scenario contains 150 "protons" but no valid star in the FOV. As required, at no time did the tracker indicate a star acquisition. If no signals were found during the search of the tracker's FOV, the highest acquisition state achieved by the tracker is the A1 state, and the minimum time to search the entire FOV is 3.8 seconds. The figure shows that the "protons" caused the search of each band to extend routinely to the A2 state, periodically to the H1 state and occasionally to the H2 state. Each state beyond the A1 state, caused by proton signals, typically adds 100 msec to the overall search time.

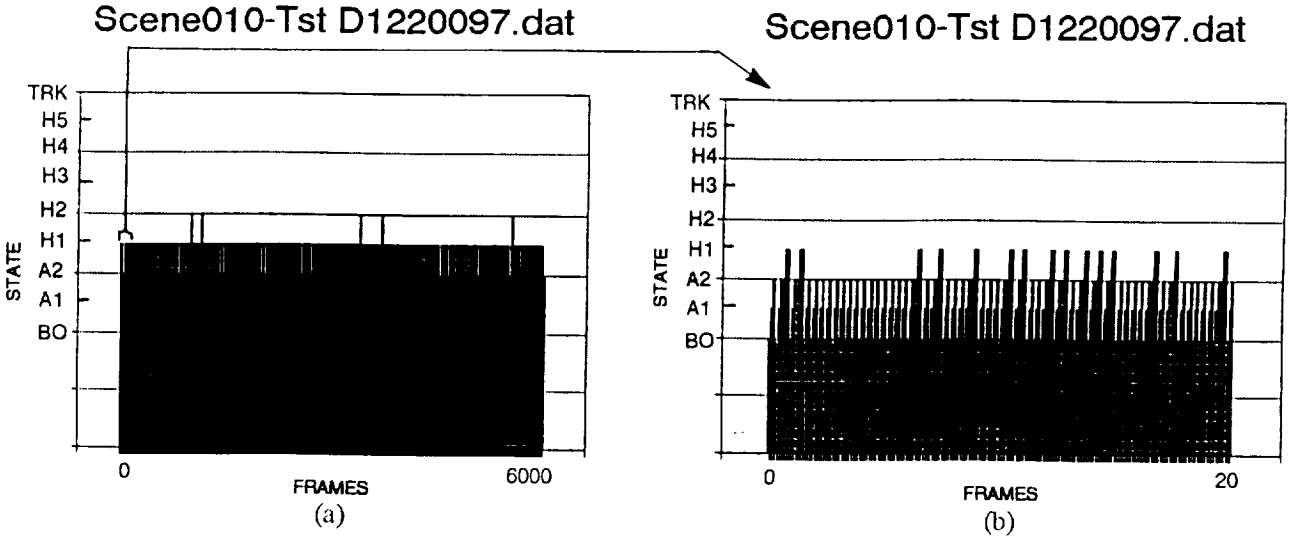


**Figure 4. The ASTRA Design Never Reports a Proton as a Star.**

Figure 5 shows the results of a test in which a "star" moves horizontally across the FOV at an apparent velocity of 0.35 degree/second and periodically experiences a direct and "near proton" hit. The figure is similar to many of the following figures. Row, Column, and Intensity are displayed as a function of tracker frame number. Row and Column are plotted in CCD pixel space, Intensity is in output counts. Any time a star signal is invalid or lost, the values of all three parameters drop to zero. A momentary dropout is characterized by a zero signal for no more than 10 frames. If the signals go to zero for more than 10 frames, the tracker has reentered the acquisition mode, and the time that the signal remains at zero is indicative of the time required to reacquire the star.

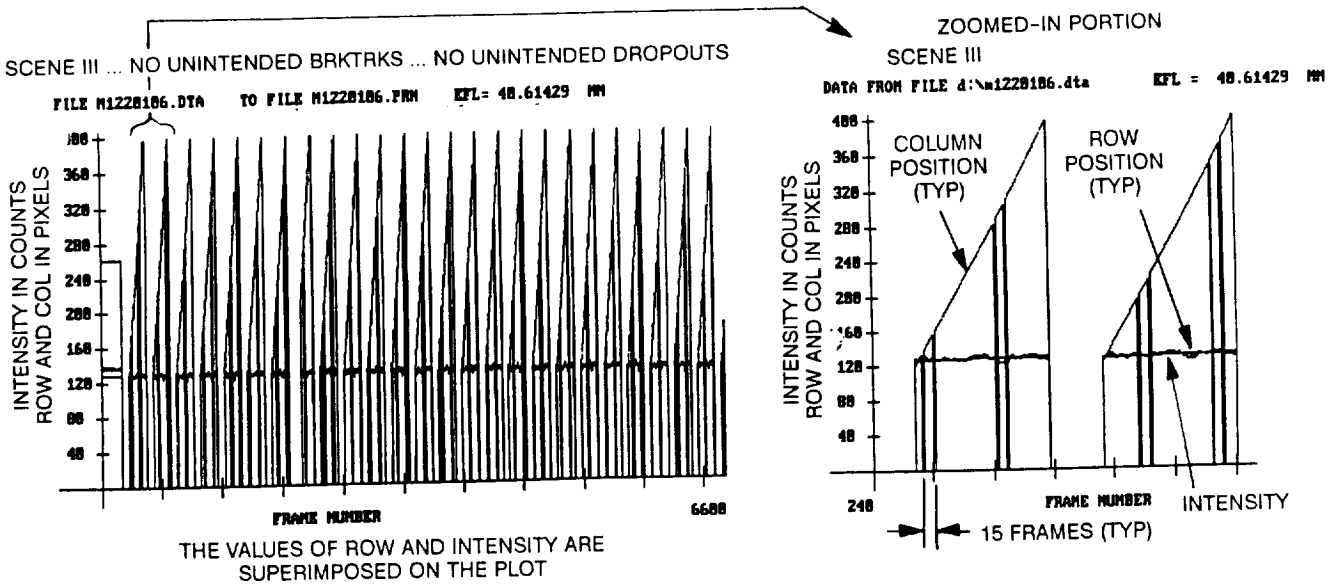


**Figure 5. ASTRA Does Not Report Star Data Corrupted by Direct or Very Near Proton Hits.**

Every 100 tracker frames, the SS causes a "proton" hit directly at the star position and 15 frames later a "proton" hit occurs 0.035 degree from the star. It can be seen from the data in Figure 5 that each event causes a dropout (i.e., the star position data is not used by the host). The increased intensity of the direct "proton" hit causes the "star" to be evaluated as invalid since its increased intensity is outside the average intensity limits being continuously determined and updated by the tracker for the valid star. The near hit, 15 frames later, drops out for the same reason since the near "proton" signal merges with the "star" signal and increases the signal intensity. If the position determination had been reported for the "near hit" condition, the position would have been in error by the bias that the "proton" signal would have introduced. For the "direct hit" condition an incorrect star magnitude would have been reported potentially impeding star identification by the host.

It was also of interest to determine how close a "proton" could come to a "star" without perturbating the star (see Figure 6). This scene has a diagonally moving star which is approached within 0.16 degree by a "proton" every 100 frames. As a benchmark, a simulated direct hit on the star by a proton was introduced causing a dropout for one frame, 15 frames prior to the near "proton" event. The data 15 frames after the dropout was reviewed and no effect of the close approach of the "proton" to the "star" was evident. View (a) of Figure 6 shows the entire test results in which the regular "star" dropouts due to the direct "proton" hit are evident. View (b) of the figure shows a single transit of the star over the tracker's FOV; view (c) shows a greatly magnified view of an area of interest. This plot is typical of all of the proton event occurrences during more than two hours of testing.

Figure 7 demonstrates the ability of ASTRA to maintain track even when a significant number of sequential frames were impacted by interfering "protons". The SS scenario was a stationary "star" interrupted by four blank scenes every 100 frames. Despite the long periodic interruptions, the tracker did not revert to the acquisition mode.

Table 1 provides statistical data on acquisition of a star in a "proton"-rich field. All the tests had either moving stars that left the FOV at one edge and then were re-introduced at the other edge or stationary stars that were deliberately caused to break-track periodically. In all but the diagonal scan cases the SS scenario was

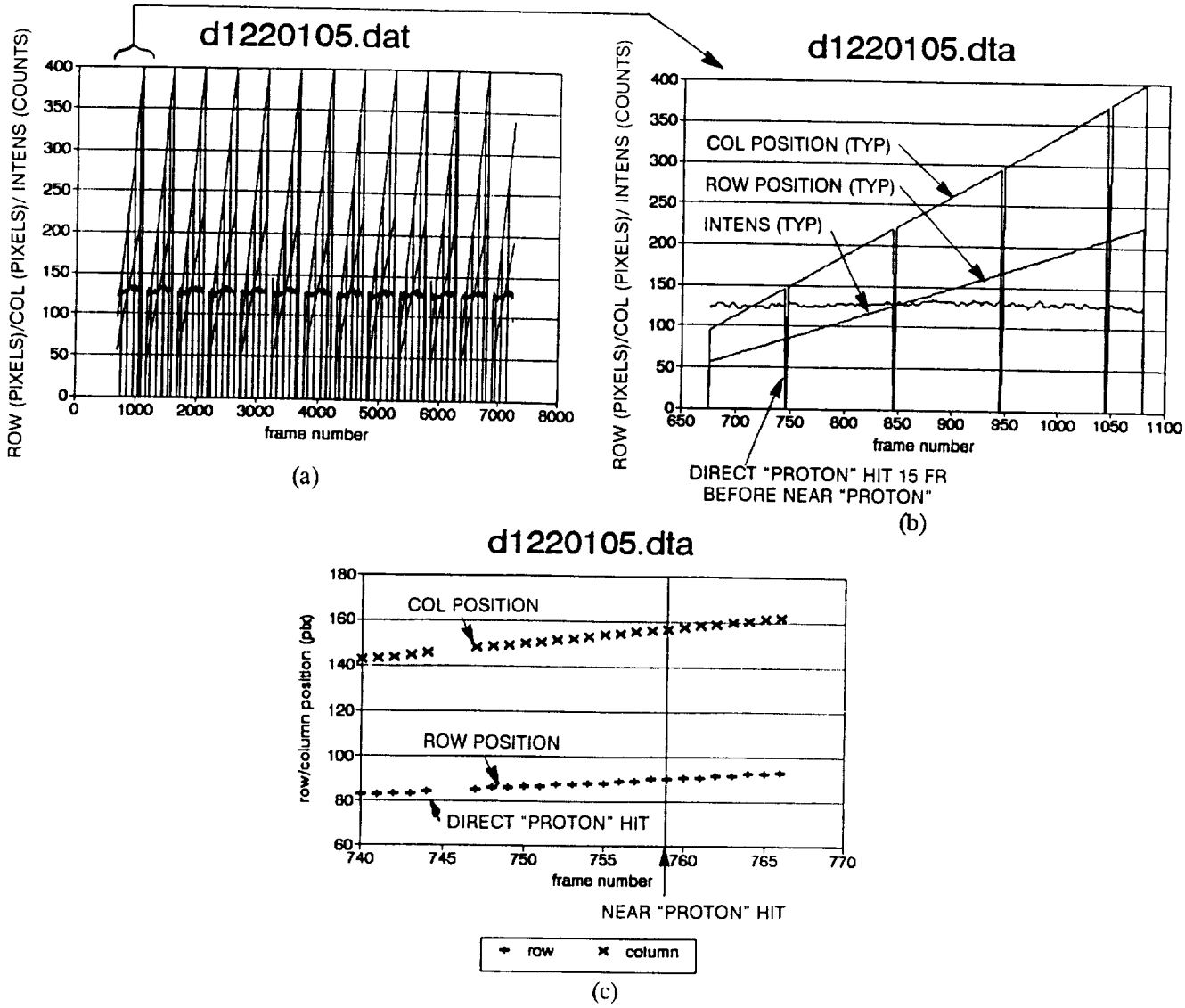


**Figure 6. ASTRA Accommodates Near (Non-Interfering) Proton Hits.**

designed so that the tracker had to search the entire FOV before it was in a position to find the star. The minimum time required to reacquire a lost star without proton interferences would be 4.4 seconds. Since the average time to acquire a star (see the table) is 7.1 seconds, the acquisition delay due to proton effects is 2.7 seconds.

## TRACKER PERFORMANCE COMPARISONS IN A PROTON FIELD

Results of tests in which the SS generates a stationary "star" positioned approximately in the center of the FOV and 150 "protons" are generated in a completely random fashion in the FOV without regard to "star" position are shown in Figures 8 through 10. Random interferences with the "star" do occur. A comparison of the data from the three tests quantitatively demonstrates the increased error in the reported "star" position due to "proton" interference with the intensity discrimination disabled (Figure 9) and with both the intensity and position discrimination disabled (Figure 10). The latter case is indicative of the performance expected from the tracker if no consideration were made in the design to accommodate proton events.

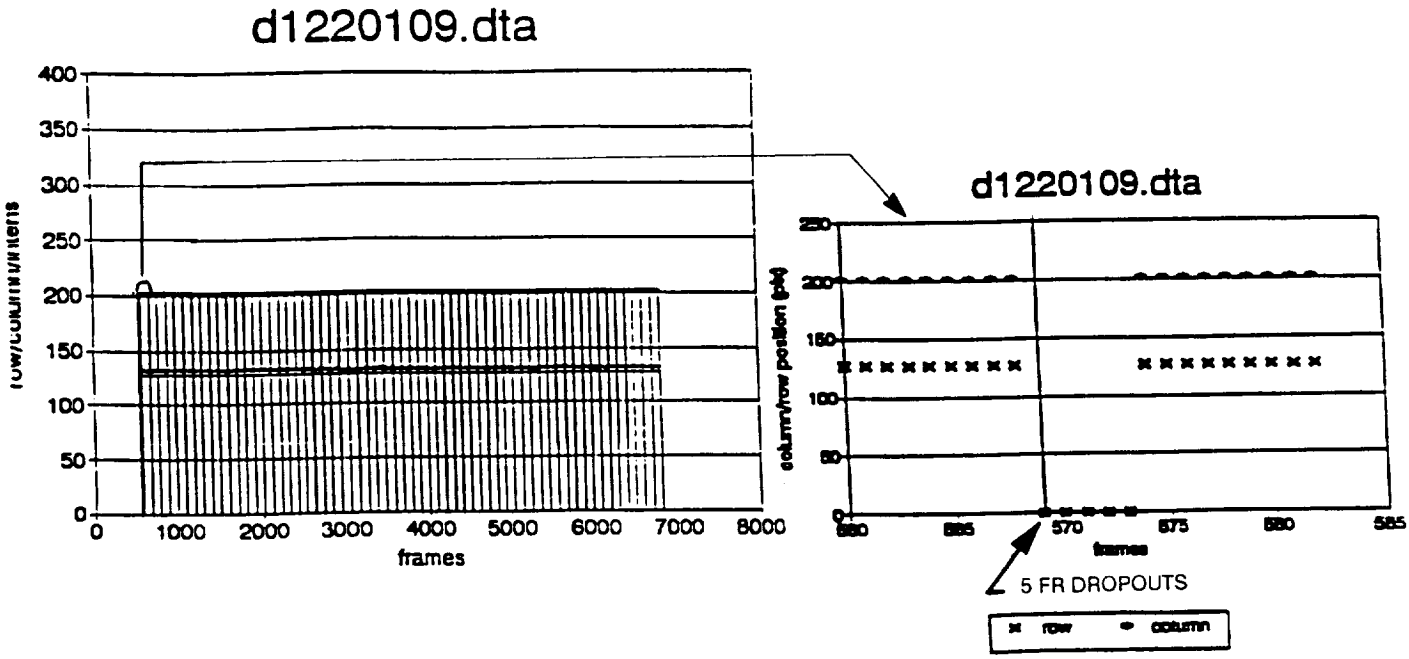


**Figure 7. Tracking of a Valid Star is Maintained for Multiple Sequential Proton Events.**

View (a) of Figure 8 illustrates the "star" position variation over an 11.6 minute test as reported by the tracker. An evaluation of the data shows that the uncorrupted data sent to the host represented 90 percent of the total number of frames. This statistic was valid for two separate trackers within 0.5 percent. This particular test displayed a standard deviation of the reported row and column positions of 5.1 arc-seconds and 3.2 arc-seconds, respectively. Figure 7(b) shows the row, column and intensity of the star plotted against time. Although there are numerous dropouts of data due to "proton" induced variations in star position or magnitude beyond preset limits, the tracker never lost the "star" long enough for the tracker to re-enter the acquisition mode.

Figure 9 presents the results from the same SS test scene but with the intensity compare discriminator disabled during the track mode. The standard deviation of the position data reported to the Host increased to 14.1 and 12.5 arc-seconds in row and column positions, respectively. Since the position comparator remains enabled the increase in the the position error is due solely to direct interference of the "protons" with the star, since the "proton" signals merge with the star signal to form an erroneous star position centroid. Despite the relatively large position errors and the numerous dropouts of "star" data, the tracker never lost the "star" to the extent that it re-entered the acquisition mode, see View (b) of Figure 9.

Figure 10 presents the results from the same SS test scene but with both the intensity compare and position compare discrimination of the tracker disabled during the track mode. The standard deviation of the reported "star" position increased to 145.3 and 173.7 arc-seconds in row and column positions, respectively. These large errors are due not only to interference with the "star" by the "protons" but, in addition, "proton" generated centroid positions are mistakenly reported as the "star" position. This case of mistaken identity

Table 1. Average Acquisition Times in "Proton" Rich Environment

| TEST IDENT | SEARCH PERIODS | TIME OF RUN(SEC) | AVG ACQ TIME(SEC) | STD DEV(SEC) | MAX TIME(SEC) | MIN TIME(SEC) | MOTION DIRECTION |
|---|---|---|---|---|---|---|---|
| T4_6_18 | 110 | 5691 | 9.2 | 2.6 | 20.3 | 7.3 | DIAGONAL |
| T2_6_13 | 139 | 7191 | 7.5 | 2.5 | 15.1 | 1.2 | DIAGONAL |
| D1220098 | 20 | 630 | 6.7 | 1.3 | 12.1 | 6.1 | STATIONARY |
| D1220101 | 20 | 639 | 6.1 | 0.16 | 6.3 | 5.8 | STATIONARY |
| D1220104 | 13 | 678 | 7.7 | 1.2 | 8.5 | 3.7 | DIAGONAL |
| D1220105 | 13 | 680 | 8.2 | 0.75 | 10.5 | 7.6 | DIAGONAL |
| D1220106 | 26 | 688 | 6.7 | 1.2 | 12.7 | 6.1 | HORIZONTAL |
| D1220121 | 25 | 646 | 6.8 | 1.3 | 12.7 | 6.1 | HORIZONTAL |
| D1210048 | 21 | 743 | 6.5 | 0.29 | 7.0 | 6.0 | STATIONARY |
| D1210051 | 20 | 672 | 6.1 | 0.18 | 6.5 | 5.8 | STATIONARY |
| D1210056 | 23 | 590 | 6.9 | 1.6 | 14.2 | 6.1 | HORIZONTAL |
| D1210057 | 26 | 714 | 6.9 | 1.4 | 13.5 | 6.1 | HORIZONTAL |

THE TOTAL NUMBER OF SEARCHES WAS_____ 456
THE TOTAL TEST TIME (HOURS) WAS_____ 5.4

THE AVERAGE ACQUISITION TIME (SECONDS) WAS____ 7.11
WITH A STANDARD DEVIATION (SECONDS) OF____ 2.00

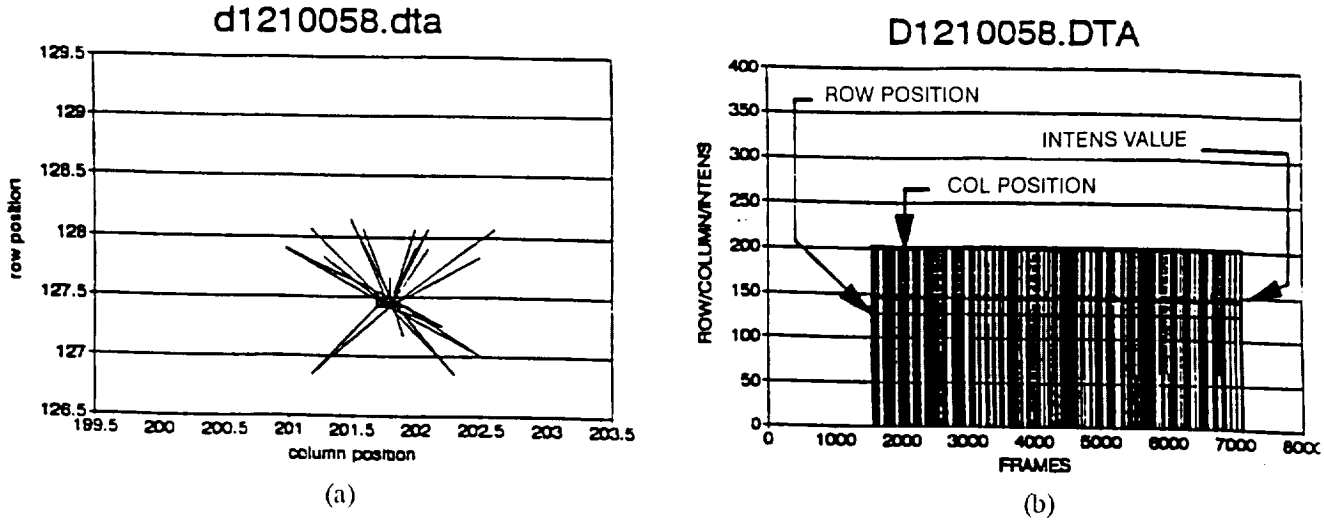


(a) (b)

Figure 8. Tracker Performance With Proton Flux Design Features. (a) "Star" Position Variations During a 10 Minute Test; and (b) Row/Col/Intensity Values Plotted Over the Test Time.

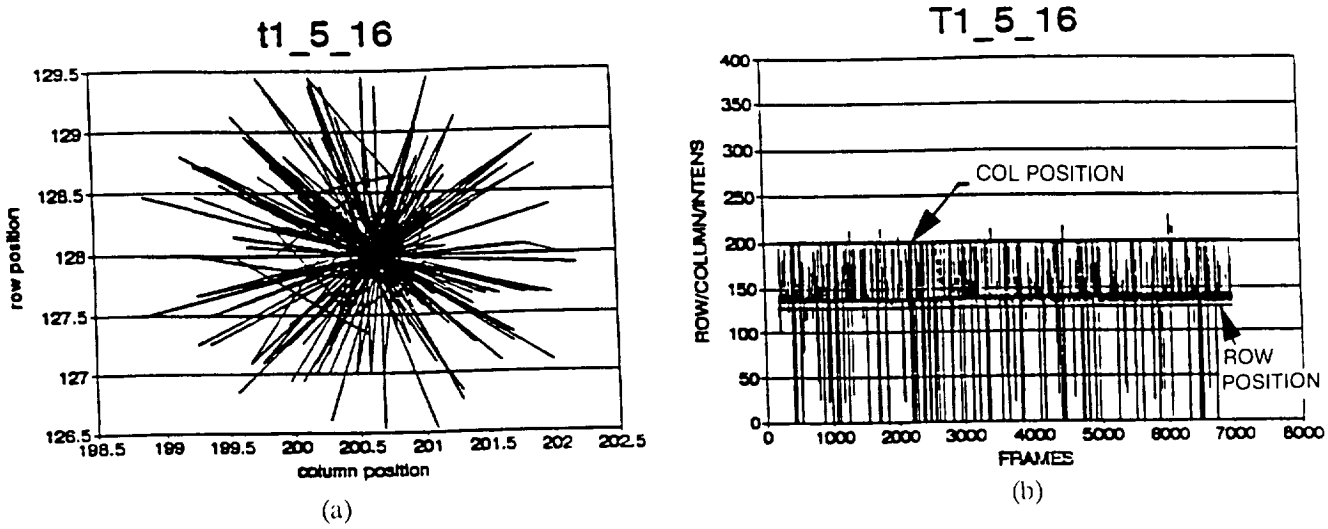


**Figure 9. Effect of "Proton" Events on Tracker Performance With Magnitude Compare Disabled. (a) "Star" Position Variation Over 11.6 Minutes Caused By "Proton" Events; and (b) Row/Col/Intensity Values Plotted Over the Test Time.**

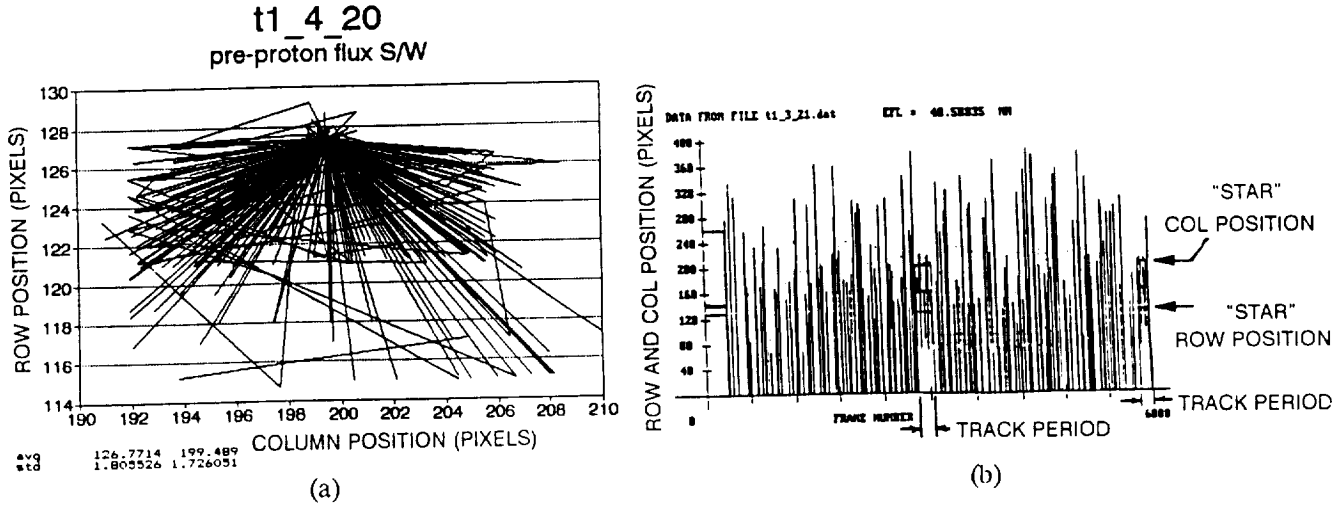


**Figure 10. Effect of "Proton" Events on Tracker Performance Without Proton-Flux Design Features. (a) "Star" Position Variation Over 30 Minutes Caused By "Proton" Events; and (b) Part of 30 Minute Test.**

occurs if the proton signal occurs within the Track Window and precedes the star position during the raster scan of the window. The dissymmetry of the "star" position variations shown in view (a) of Figure 10 is explained by this phenomena. View (b) shows a case in which the errors have become so large that the "star" is lost and the tracker must re-enter the acquisition mode to re-acquire the "star".

Figure 11 evaluates the same data from an acquisition perspective. The software of the tracker with the position and magnitude comparators disabled was also modified so that during acquisition the first signal with the characteristics of a valid star (i.e., proper size and magnitude) would cause a transition to track. (The multiple frames and tests implemented in the design for use in high-proton flux environments were disabled.) In the proton-rich environment, as simulated here, a large number of false star acquisitions were caused by proton signals. The actual "star" was acquired only nine times in 30 minutes of tracker operation, and was tracker for only six percent of the time.

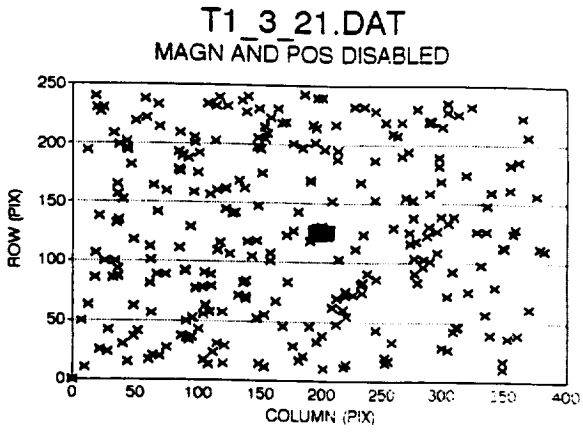


**Figure 11. Without the Proton Flux Design Features, the Tracker Will Usually Acquire and Attempt to Track Proton Events.**

## SUMMARY

Radiation-induced proton events can result in anomalous operation of solid-state star trackers, specifically:

- Erroneous acquisition of proton events and/or failure to acquire valid stars
- Loss of track of valid stars
- Incorrect position and intensity data.

Through incorporation of hardware-efficient processing algorithms, HDOS has completed delivery of two flight trackers for the TOPEX/Poseidon mission which can operate effectively in a proton-rich environment. Using a scene simulator to produce effects similar to those caused by protons, tests validating the performance gains achieved have been completed on both units. For an environment that produces 150 false multi-pixel events at the detector, the following results were obtained:

- No acquisition of false stars (proton events)
- Reliable acquisition of valid stars
- No loss of tracking a valid star
- Identification of corrupted data for the host, caused by proton impact upon valid star pixel groups.

The algorithms incorporated into the tracker firmware can be tailored to unique user mission requirements. The scene simulation techniques developed provide a powerful tool for validating performance for rather unique and complex test conditions.

## REFERENCES

1. H. L. Fisher, T. E. Strickwerda, C. C. Kilgus, L. J. Frank, "Autonomous, All-Stellar Attitude Determination Experiment: Ground Test Results" "Autonomous Star Sensing and Attitude Determination", AAS 91-025, 1991.

2. R. Rau, "Space Radiation, Protons, and CCDs" HDOS TechNews vol. 2 iss 6, December 1991.

3. E. G. Stassinopoulos, J. P. Raymond, "The Space Radiation Environment for Electronics" Proc. IEEE, vol. 76, no. 11, Nov. 1988.

4. J. Janesick, T. Elliott, F. Pool, "Radiation Damage in Scientific CCDs" IEEE 1988 Nuclear Science Symposium, Orlando FL.

5. T. Lomheim, R. Shima, J. Angione, W. Woodard, D. Asman, R. Keller, L. Schumann, "Imaging CCD Transient Response to 17 and 50 MeV Proton and Heavy-Ion Irradiation" (preprint submitted to IEEE Trans. on Nuclear Science).

6. F. Kubick, "Statistical Aspects of CCD Radiation Noise", (HDOS internal memo).

7. B. Bloom, "TOPEX Star Tracker 'False' Star Contour Maps", presented to Fairchild TOPEX Attitude Control Group, July 12, 1990.